ELSEVIER

Polymer 44 (2003) 2919–2925

polymer

www.elsevier.com/locate/polymer

Conformational and dynamo-optical properties of fluorinated poly(*p*-phenylene-1,3,4-oxadiazole-imide-amide) molecules in solutions

Peter Lavrenko[a,*], Olga Okatova[a], Irina Strelina[a], Maria Bruma[b], Burkhard Schulz[c]

[a]*Institute of Macromolecular Compounds, Russian Academy of Sciences, Bolshoy pr., 31, St. Petersburg 199004, Russian Federation*
[b]*Institute of Macromolecular Chemistry, Romanian Academy of Sciences, Iasi 6600, Romania*
[c]*Institut für Dünnschichttecnologie und Mikrosensoric e. V. Teltow, 14513 Teltow, Germany*

Received 21 August 2002; received in revised form 10 February 2003; accepted 19 February 2003

Abstract

Conformational parameters of the fluorinated poly(*p*-phenylene-1,3,4-oxadiazole-imide-amide) molecules in dilute solutions in *N*,*N*′-dimethylacetamide, *N*,*N*′-dimethylformamide and 96% sulphuric acid were evaluated by using the data of hydrodynamic and dynamo-optical investigations. Optical anisotropy of the statistical Kuhn segment was found to be about half of that for poly(amide-benzimidazole) and close to that previously obtained for poly(*p*-phenylene-1,3,4-oxadiazole) molecules. The observed effect is referred to the higher equilibrium flexibility of the polymer chain attributed to the hexafluoroisopropylidene units incorporated into the molecule backbone. Noticeable degradation of the polymer molecules in solution in 96% H_2SO_4 at ambient temperature was detected and characterised.

Keywords: Conformation; Flexibility; Optical anisotropy

1. Introduction

Most of the aromatic polyamides, polyimides, polybenzazoles and other heterocyclic polymers are well known as high-performance polymer materials for their excellent mechanical and electrical properties, and high thermal stability. The peculiar specificity of these wormlike polymers is rather high equilibrium rigidity of the chains, which is determined by original structure of the macromolecules. Therefore, supra-molecular structure and mechanical properties of the polymers are mainly provided by extended conformation of the individual macromolecules [1–4]. They are poly(*p*-phenylene terephthalamide) (Trade Mark 'Kevlar'), poly(*m*-phenylene isophthalamide), poly(*p*-phenylene)s, and a set of heterocyclic polymers such as poly(amide benzimidazole), poly(naphthoylene imide benzimidazole), poly(oxadiazole)s, poly(oxaphenyl benzoxazole terephthalamide)s, and many others [5–17].

At the same time, these polymers are often intractable substances, which do not melt before thermal decomposition, and are insoluble in routine organic solvents. Copolymerisation and incorporation of a flexible spacer are the advanced practical methods to improve the solubility of the polymer and to decrease its melting point.

Recently, by the methods of molecular hydrodynamics and dynamo-optics, we have investigated the conformational and optical properties of the molecules of naphthalene modified poly(1,3,4-oxadiazole) [18] and poly(phenylene-1,3,4-oxadiazole) (POD) copolymers with *meta*- and *para*-phenylene cycles regularly alternated along the polymer chain [19]. These advanced polymers have a combination of good properties in manufacturing the materials for special applications such as excellent thermal and hydrolytic stability, good mechanical behaviour, dielectric and electroluminescence properties [20,21]. The present work deals with the investigations of a new POD derivative polymer, namely, fluorinated poly(*p*-phenylene-1,3,4-oxadiazole-imide-amide) (PODIA), in dilute solutions using the same methods: translational diffusion, flow birefringence (FB), and viscometry.

The chemical structure of the polymer repeat unit is as follows (Scheme 1).

Fluorinated heterocyclic polymers [22,23], such as this one, have the better dielectric characteristics and also better solubility and compatibility. The polymer is readily soluble

* Corresponding author. Tel.: +7-812-328-8529; fax: +7-812-328-6869.
E-mail address: lavrenko@mail.macro.ru (P. Lavrenko).

0032-3861/03/$ - see front matter © 2003 Elsevier Science Ltd. All rights reserved.
doi:10.1016/S0032-3861(03)00172-1

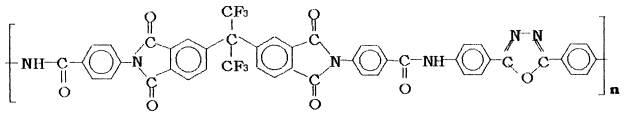

PODIA

Scheme 1.

in amide solvents and in *N*-methylpyrrolidinone (N-MP) in contrast to many heterocyclic polymers which are soluble only in such proton-donor solvents as concentrated sulphuric acid. Thus, with PODIA we had a good opportunity of comparative investigation in both protonic and aprotic solvents.

2. Experimental

The PODIA sample was prepared by low-temperature polycondensation of the equal-molar amounts of diamino oxadiazoles and diacid chlorides in N-MP in solution at the concentration 5–10%, using pyridine as an acceptor [24,25]. The sample was dried at ambient temperature till the constant weight.

Solutions were prepared in *N*,*N*′-dimethylacetamide (DMA) and *N*,*N*′-dimethylformamide (DMF) 1 day before the measurements. Preparation of the solutions in sulphuric acid is detailed in the text. A particular lot of 96% sulphuric acid was used as a solvent with viscosity of $\eta_0^{26} = 18.26 \times 10^{-2}$ g/cm s, a density $\rho_0 = 1.8285$ g/cm^3, and refractive index of $n_D = 1.4375$. For DMF they were $\eta_0^{26} = 0.787 \times 10^{-2}$ g/cm s, $\rho_0 = 0.9426$ g/cm^3, and $n_D = 1.4270$, for DMA $\eta_0^{26} = 0.937 \times 10^{-2}$ g/cm s, $\rho_0 = 0.9380$ g/cm^3, and $n_D = 1.4358$.

Viscometry and diffusion measurements and the FB technique specially developed for the corrosive and hydroscopic solvents were used as had been described earlier [18,19]. The solution viscosity was measured at 26 °C with an Ostwald type viscometer under conditions where the gradient dependence of viscosity was absent and the kinetic energy effect was negligible. Free translational diffusion was investigated at 26 °C with the Tsvetkov polarizing diffusometer [11] of convectional type in a Teflon cell 2.0 cm thick (*h*) [26]. The spar twinning *a* was 0.10 cm, and the interference fringes period of a compensator *b* was 0.15 cm.

The FB experiments were performed at 21 °C in a co-axial cylindrical dynamo-optimeter with an inner rotor of radius *R*, length *l*, and with a gap ΔR. The FB measurements were carried out with varying the flow rate gradient in the gap *g* ($g = 2\pi R\nu/\Delta R$), through the variation of the rotor revolution frequency ν (s^{-1}) within the laminar regime ($g \leq g_{lim}$). Here g_{lim} is the upper gradient limit for laminar flow in a liquid with viscosity η and density ρ defined by $g_{lim} = 41.3(R/\Delta R^5)^{1/2} \times (\eta/\rho)$. Solutions in sulphuric acid were investigated in a Teflon dynamo-optimeter (with $R = 2.3$ cm, $l = 5.9$ cm, $\Delta R = 0.061$ cm, $g_{lim} = 3600$ s^{-1}). Solutions in organic solvents were investigated in a Titanium dynamo-optimeter (with $R = 1.84$ cm, $l = 3.0$ cm, $\Delta R = 0.030$ cm, $g_{lim} = 6700$ s^{-1}). Under the laminar flow conditions, the data obtained were independent of the dynamo-optimeter parameter sets.

Birefringence Δn induced in the flow shear field was determined by the visual compensation optical system [11] with the penumbral plate. Thin mica plates with an optical path difference $\delta_k/\lambda = 0.019$ or 0.0389 (λ is the light wave length) were used as a Brice-type compensator. Δn was calculated using $\Delta n = (\delta_k/l)\sin 2\varphi$, where φ is the azimuth angle of the compensator as fixed at given *g*. The light source was Hg lamp ($\lambda = 546.1$ nm).

3. Results and discussion

3.1. Hydrodynamic properties

The intrinsic viscosity $[\eta]$ was calculated in the usual way from the *c* dependence of the inherent viscosity, η_{sp}/c, as illustrated by the points in Fig. 1. It was approximated by a linear function in accordance with the Huggins' equation $\eta_{sp}/c = [\eta] + k_H[\eta]^2 c$ where k_H is the Huggins' constant. The close $[\eta]$ and k_H values were obtained in DMF and DMA (curves 1 and 2, respectively). The results are given in Table 1.

Diffusion coefficient was calculated by $D = (1/2)\partial\bar{\sigma}^2/\partial t$ from the diffusion boundary dispersion, $\bar{\sigma}^2$, plotted against time. Symmetrical interference fringes were treated in Gaussian approximation. In this way, the dispersion $\bar{\sigma}^2$ was obtained using the formula $\bar{\sigma}^2 = (a^2/2^3)/[\text{argerf}(aH/Q)]^2$ where argerf is the argument of the probability integral, *H* the maximum ordinate and *Q* the interference fringe area. Diffusion experiments were characterised with the linear dependence of $\bar{\sigma}^2$ on *t* (points 1 in Fig. 2) throughout the experiment, without decreasing the slope with time coursed

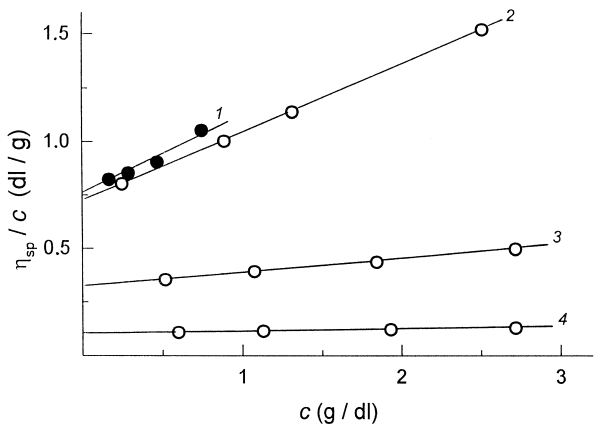

Fig. 1. Concentration dependence of η_{sp}/c for PODIA in (1) DMF, (2) DMA, and (3) and (4) 96% H_2SO_4 at 26 °C. Points 3 and 4 were obtained within 1 and 15 days of the solution storage.

Table 1
Hydrodynamic and dynamo-optical properties of PODIA in solution

Solvent	DMA	DMF	96% H_2SO_4
$[\eta]$ (dl/g)	0.75	0.74	0.32
k_H	0.58	0.54	0.62
$(dn/dc)_{546}$ (cm^3/g)	–	0.17 ± 0.02	0.20 ± 0.05
$D \times 10^7$ (cm^2/s)	–	5.6	0.32
$M_{D\eta} \times 10^{-3}$ (g/mol)	–	14 ± 3	19 ± 5
$(\Delta n/\Delta\tau)_{M\to\infty} \times 10^{10}$ (cm s^2/g)	66	–	110

by sample heterogeneity. This is in accord with the fact that PODIA belongs to the condensation polymers with the typical $M_w/M_n \leq 2$ values. The D value of $(5.6 \pm 0.3) \times 10^{-7}$ cm^2/s was thus obtained for PODIA in DMF. The concentration effects were negligible at the solute concentration used ($c \leq 0.18$ g/dl).

The interference fringe area was used also to evaluate the refractive index increment $(dn/dc)_{546}$ by $dn/dc = (\lambda/abh)Q/c$ where λ is the light wave length and the other symbols are defined above (in Section 2). The $(dn/dc)_{546}$ value of (0.17 ± 0.02) cm^3/g was found for PODIA in DMF and 0.20 cm^3/g in 96% H_2SO_4.

Molecular weight was determined from the diffusion-viscometric data by [27]

$$M_{D\eta} = 100(A_0 T/D\eta_0)^3/[\eta] \quad (1)$$

on the assumption that the hydrodynamic parameter A_0 is independent of M for the polymer investigated. Here T is the Kelvin temperature. The 3.6×10^{-10} erg/K $mol^{1/3}$ value was used for the invariant A_0 as being the value typical for rigid-chain polymers [27] and confirmed by the data on poly(*p*-phenylene-1,3,4-oxadiazole) (PPOD) in the same solvent [16]. The $M_{D\eta}$ value of $(14 \pm 3) \times 10^3$ g/mol was thus obtained, and the degree of polymerisation 16 ± 3.

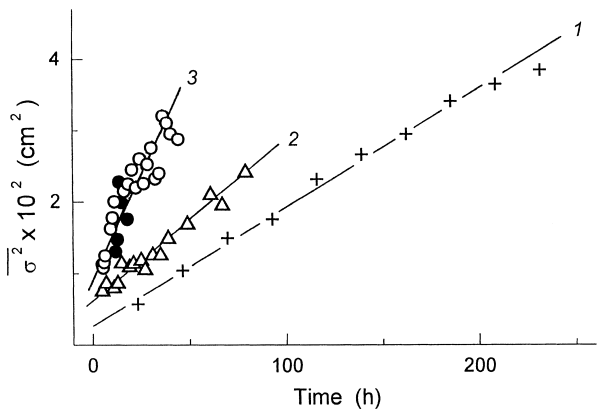

Fig. 2. Dispersion $\bar{\sigma}^2$ of diffusion boundary versus time as obtained for PODIA in solution in (1) DMF and (2) and (3) in 96% H_2SO_4 at 26 °C. Solute concentration c = (1) 0.183, (2) 0.134, (3, open points) 0.076, and (3, filled points) 0.067 g/dl. Points 2 and 3 were obtained within 1 and 15 days of the solution storage; open and filled points (3) represent the data of independent measurements. For points 1, the t value was taken as $t \times (\eta_0^{suph.ac.}/\eta_0^{DMF})$.

3.2. Equilibrium rigidity of macromolecule

The chain flexibility of heterocyclic polymers was shown to be determined mainly by the structural mechanism of flexibility [19]. Therefore, the degree of coiling of the PODIA macromolecule was evaluated from the comparison of conformational and optical PODIA properties with those for the polymers of similar structure. Particularly, PODIA properties were compared with those of PPOD, poly(amide benzimidazole) (PABI) and poly(tetra-phenylmethane terephtalamide) (PTPMTPA). These polymers were previously investigated over the wide range of M [7,28,29]. The repeat units of PPOD, PABI, and PTPMTPA are shown below (Scheme 2). Valence angles and distances were taken from the paper [30].

It is easy to see that in the PODIA structural (repeat) unit, after two units like that of PABI linked one to another as 'head to head' by one methylene group, there come the PPOD unit and the *p*-phenylene cycle. The last one does not change the direction of the axis of intramolecular rotation but elongates the unit only. The type of the PABI units linkage (head to head or 'head to tail') was shown not to influence markedly the macromolecule conformation [31]. Therefore, in accordance with the principle of additivity of flexibility mechanisms, the expected number of the structural units s in the Kuhn segment for the PODIA macromolecule (s is clear to be the characteristic parameter of correlation in the space orientation of the macromolecule units) was calculated by

$$s = [(2/s_1) + (0.5/s_2) + (1/s_3)]^{-1}$$

where s_1, s_2, and s_3 are the partial s values known for PABI, polyethylene and PPOD. Substituting here the experimental values $s_1 = 11$, $s_2 = 8.3$, and $s_3 = 11$ [7,28,32] we obtain $s = 3.0$. The segment length $A = s \times \lambda$ where λ is the PODIA repeat unit length along the macromolecule axis. Using $\lambda = 36.2$ Å, we obtain $A = 109$ Å.

The relatively large segment length allows to classify PODIA as a polymer with the semi-flexible macromolecules whose preferable conformation is intermediate between rod

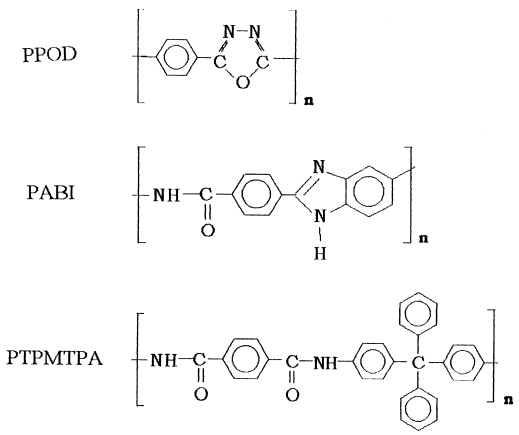

Scheme 2.

and draining coil. The contour length of the PODIA macromolecule consists of approximately five segments, and the large segment length is obviously due to large length of the repeat unit (36.2 Å) rather than by high number of the units in the segment ($s = 3$) when compared with the $s = 6-8$ value as typical for many flexible-chain polymers [11].

It is interesting to compare the conformational parameters, thus obtained for PODIA, with the characteristics of the structural chain flexibility, which can be evaluated theoretically from the geometrical structure of the macromolecule. This flexibility is determined by the length of the chain linear parts and by the structural mechanisms which disturb the co-axial internal rotations. Let enumerate these mechanisms for the PODIA chain as (1) inequality of valence angles at carbon and nitrogen atoms, (2) thermal disturbances of the amide group coplanarity and (3)–(5) kinks of the chain at the points of disposition of the (3) benzimide, (4) methylene, and, at last, (5) oxadiazole units. Schematically, this is represented below (Scheme 3). As a result, the PODIA molecule can be modelled by the chain of virtual bonds, in which the displacement for one repeat unit is accompanied by the kinks of the internal rotation axis for the angles $\vartheta_1 = 10°$(twice), $\vartheta_2 = 20°$(twice), $\vartheta_3 = 30°$(twice), $\vartheta_4 = 70.5°$, and $\vartheta_5 = 46.6°$, respectively [15,29,30,33].

The number of the repeat units s in the Kuhn segment was evaluated by the expression (2) valid for the equivalent chain with the angle ϑ between the bonds of rotation when the hindrance to the intramolecular rotation is characterised by parameter σ [34]

$$s = \sigma^2 \frac{1 + \cos\vartheta}{1 - \cos\vartheta} \Big/ \left(\cos\frac{\vartheta}{2}\right)^2 \tag{2}$$

Substituting ϑ_i in Eq. (2) we obtain $s_3 = 14.9$ and $s_4 = 3.0$.

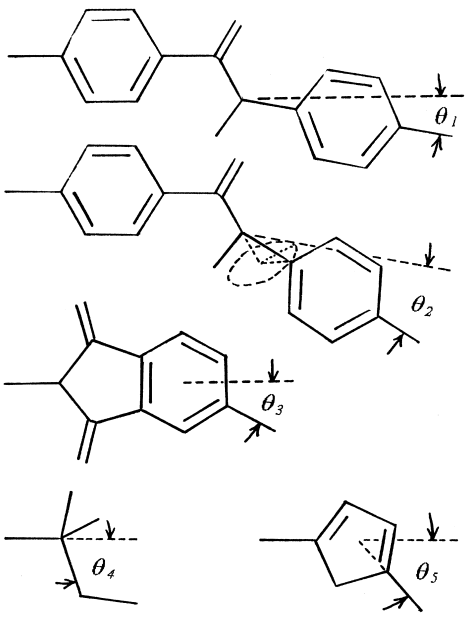

Scheme 3.

The $s_1 = 130$, $s_2 = 44$, and $s_5 = 6.4$ values were obtained earlier [16].

The principle of additivity known for structural mechanisms of flexibility was also used as confirmed for PPOD previously [18,19]. For the PODIA model chain with free internal rotation ($\sigma = 1$), this principle is described by the equation

$$s_{fr} = [(2/s_1) + (2/s_2) + (2/s_3) + (1/s_4) + (1/s_5)]^{-1}$$

where the lower index indicates the corresponding flexibility mechanism and the multiplier 2 allows for the presence of two amide groups and two benzimide circles in the chain repeat unit. As a result, for the PODIA model chain we obtain $s_{fr} = 1.46$ and the Kuhn segment length $A_{fr} = s_{fr}\lambda = 53$ Å. The parameter of hindrance to internal rotations σ in the real macromolecule was evaluated by using Eq. (2): $\sigma = (A_{calc}/A_{fr})^{1/2} = 1.5$.

This value is close to σ known for PPOD ($\sigma = 1.3$), poly(*p*-phenylene terephthalamide) (1.4) [16], and PTPMTPA (1.5) molecules [29]. The result is not surprising because the tetraphenyl-methane groups, inserted into PTPMTPA molecular chain, prevent rotational bonds to be parallel and also distort the chain for a tetrahedron angle. The equilibrium flexibility of the PODIA chain is considerably (for about a half) determined by this mechanism.

These correlations provide an evidence that the principle of structural flexibility can be surely applied to conformational analysis of the PODIA molecules.

3.3. Flow birefringence

Fairly large and positive (in sign) birefringence Δn was observed in solutions of PODIA in DMA and 96% H_2SO_4 subjected to the flow field. The effect observed in neat solvent was negligible (less than 1% of that in solution). Therefore the Δn value measured in the solution can be considered as over birefringence, which is the characteristic of the solved polymer. At any solute concentration, Δn was found to depend linearly on the shear rate g (Figs. 3 and 4) that is a typical result for a real solution. This permits to characterise the effect with the relation $\Delta n/g$ and to evaluate the shear optical coefficient $\Delta n/\Delta\tau$ defined by the expression $\Delta n/\Delta\tau = \lim_{c\to 0} \lim_{g\to 0} \Delta n/gc(\eta - \eta_0)$. Here $\Delta\tau$ is the over shear stress and η the solution viscosity. As a result, we obtained the $\Delta n/\Delta\tau$ value of 55×10^{-10} cm s^2/g for PODIA in DMA and the higher value, 92.5×10^{-10} cm s^2/g, in 96% H_2SO_4.

The dependence of $\Delta n/\Delta\tau$ on molecular weight for a kinetically rigid chain is well approximated by the expression [11]

$$\Delta n/\Delta\tau = (\Delta n/\Delta\tau)_{M\to\infty} M/(M + M_0 s)$$

where $(\Delta n/\Delta\tau)_{M\to\infty} = \lim_{M\to\infty} \Delta n/\Delta\tau$, M_0 is the mass of monomer unit, and s the number of monomer units in the segment. Substitution of $M_0 = 898.8$ g/mol and $s = 3$ leads

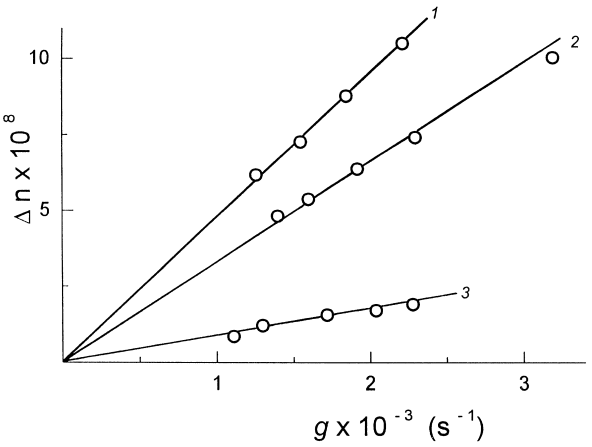

Fig. 3. Flow birefringence Δn versus flow shear rate g as observed in PODIA solution in DMA at 21 °C. Solute concentration is (1) 0.86, (2) 0.60, (3) 0.25 g/dl.

to the $(\Delta n/\Delta\tau)_{M\to\infty} \times 10^{10}$ value of 66 and 110 cm s^2/g for PODIA in DMA and 96% H_2SO_4, respectively.

The latter is markedly lower than that previously obtained for PPOD in the same solvent (i.e. 135×10^{-10} cm s^2/g [35]). Taking into account the close values of refractive index increment obtained for these polymer–solvent systems, we may conclude that the form-effects [11] contribute the same part into the FB effects observed in the solutions of both polymers under discussion. In addition, the macro-form effect is negligible here as in the case of the other PPOD derivatives [16,18,19].

Optical anisotropy Δa of the chain segment can be determined by

$$(\Delta n/\Delta\tau)_{M\to\infty} = B\Delta a \quad (3)$$

where $B = (4\pi/45kTn)(n^2+2)^2$, kT is the thermal energy, and n the refractive index of the solvent. Substituting $(\Delta n/\Delta\tau)_{M\to\infty} = 110 \times 10^{-10}$ cm s^2/g into Eq. (3) we obtain

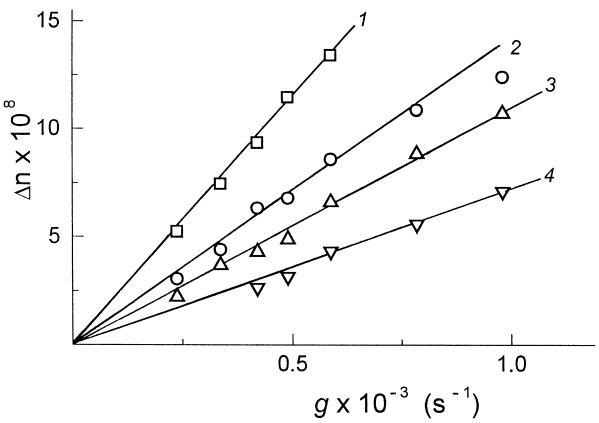

Fig. 4. Flow birefringence Δn versus flow shear rate g as observed in PODIA solution in 96% H_2SO_4 at 21 °C. Solute concentration is (1) 0.29, (2) 0.22, (3) 0.21 and (4) 0.14 g/dl.

$\Delta a = 1400 \times 10^{-25}$ cm^3 for PODIA in 96% H_2SO_4. The micro-form effect was evaluated by [11]

$$(\Delta a)_f = (dn/dc)^2 M_0 s/2\pi N_A \bar{v}$$

where $\bar{v}$ is a partial specific volume of the solute in solution. Using $\bar{v} = 0.7$ cm^3/g, experimental values of dn/dc (0.20 cm^3/g), and s obtained above we have $(\Delta a)_f = 400 \times 10^{-25}$ cm^3. The consideration of the $(\Delta a)_f$ will give a proper optical anisotropy of the Kuhn segment $(\Delta a)_{pr} = \Delta a - (\Delta a)_f = 1000 \times 10^{-25}$ cm^3. Optical anisotropy per chain unit length is $\beta = (\Delta a)_{pr}/A = 13.0 \times 10^{-17}$ cm^2.

This value lies within the range of the β values obtained for the POD *para*- and *meta*-isomers $\{(16-11) \times 10^{-17}$ cm^2 [16]$\}$ and is 1.4 times less than that of PABI (18×10^{-17} cm^2 [36]). The last result should be referred to the presence of the optically isotropic hexafluoroisopropylidene groups. A similar effect was previously observed for PTPMTPA molecules [29].

Note, the value of the optical parameter B in Eq. (3) for PODIA in DMA is close to that in 96% H_2SO_4 (7.86×10^{13} and 7.92×10^{13}, respectively). Hence, the difference in the experimental $\Delta n/\Delta\tau$ values observed in the present work means that Δa for the PODIA molecule in DMA is significantly lower than that in 96% H_2SO_4. The similar interesting result was earlier obtained for PABI, where, over the Gaussian range of M, the $(\Delta n/\Delta\tau)_{M\to\infty}$ values were of 280×10^{-10} and 360×10^{-10} cm s^2/g in organic solvent and in sulphuric acid solutions, respectively [36].

3.4. Properties in sulphuric acid and degradation

One can see that hydrodynamic properties of the PODIA molecules in DMF are similar to those in DMA (Table 1). Now we turn to the comparison of these properties with the viscometric and diffusion data obtained in 96% H_2SO_4 and illustrated by curves 3 and 4 in Fig. 1 and curves 2 and 3 in Fig. 2. We have to note that the concentration boundary in diffusion experiment in this solvent was hydrodynamically unstable at low polymer concentrations ($c \leq 0.1$ g/dl). Therefore, the solution properties were investigated here at elevated concentrations and then extrapolated to $c = 0$. As a result, in 96% H_2SO_4 we have obtained $[\eta] = 0.32$ dl/g, $D = 0.32 \times 10^{-7}$ cm^2/s, and $dn/dc = 0.20 \pm 0.03$ cm^3/g. Using Eq. (1) we obtain $M_{D\eta} = (19 \pm 5) \times 10^3$ g/mol, which coincides well with that in DMF. This is due to the fact that the $[\eta]$ value in 96% H_2SO_4 is approximately a half of that in DMF whereas the $(D\eta_0)$ value is 1.33 times higher. Hence, on the first stage of dilution, the polymer forms a real (molecularly dispersed) solution in both DMF and DMA, as well as in 96% H_2SO_4.

However, the PODIA solution in 96% H_2SO_4 was found to be unstable in time as this is shown in Fig. 5. The relative viscosity of the solution first increases (indicating the dissolution process) but after 1.5 h it decreases unceasingly (and irreversibly). After the solution storage for 14 days at

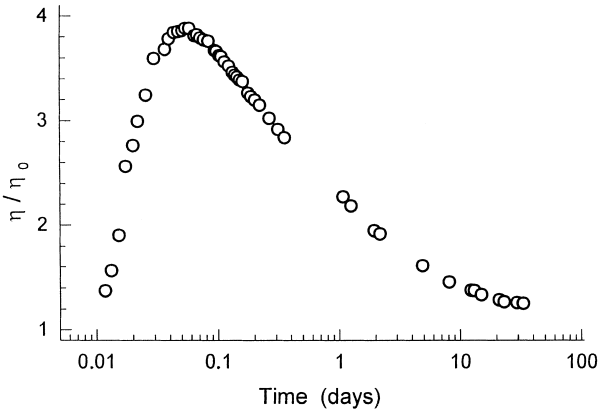

Fig. 5. Time dependence (in semi-logarithmic scale) of reduced viscosity η/η_0 for PODIA solution in 96% H_2SO_4 at 21 °C. Solute concentration is 3.4 g/dl.

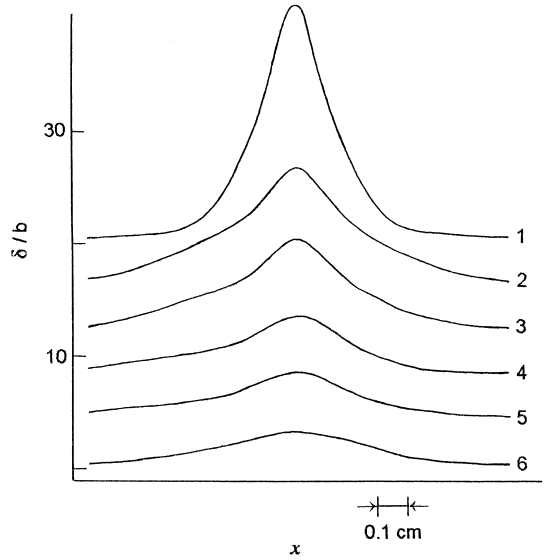

Fig. 6. Evolution of the diffusion profile trace (represented in the number of interference fringes, δ/b) with time as observed for PODIA in 96% H_2SO_4 at 26 °C within 15 days of the solution storage. For convenience, every second curve is here shifted down for four units. Solute concentration is 0.076 g/dl. Pictures were registered within 2, 7, 10, 16, 24, and 42 h (downward) after the experiment start-up.

ambient temperature, the intrinsic viscosity falls to one-third of its original value (curves 3 and 4 in Fig. 1). Simultaneously, the diffusion coefficient increases approximately twice (as obtained from curves 2 and 3 in Fig. 2), and the molecular weight falls to 5×10^3. These data indicate the degradation of PODIA molecules in 96% H_2SO_4 that may be described in terms of the degradation rate constant k defined by $P^{-1} = P_0^{-1} + (kt/2)$. Here P_0 and P is the degree of polymerisation for the initial sample and for the sample at time t, respectively, and t (in min) is the time of degradation. At ambient temperature, the k value was found to be 1.3×10^{-5} min^{-1}. The rate of PODIA degradation in 96% H_2SO_4 is obviously significant but several times lower than that observed earlier for the aromatic polyamic acid molecules under the same conditions ($k = 8 \times 10^{-5}$ min^{-1} [37]).

In addition, the several-fold decreasing in the diffusion curve area during the diffusion process of PODIA molecules in 96% H_2SO_4 (after the storage of the solution for 2 weeks) and the non-Gaussian form of each curve in Fig. 6 may be attributed to the inhomogeneity of the polymer sample increasing with time. This fact also explains the higher scattering of the experimental points about curve 3 in Fig. 2 (as compared with curve 2).

4. Conclusions

In this study, it has been demonstrated that the insertion of the hexafluoroisopropylidene groups into the backbone of semi-rigid polyheteroarylene leads to higher coiling of the macromolecule in the isolated state. This is close to the effect previously observed for *p*-aromatic polyamide when tetraphenyl-methane groups were inserted into the polymer chain. Hence, the structural mechanism of chain flexibility is the main mechanism that determines the conformation of PODIA molecules in solution.

The shear optical coefficient $\Delta n/\Delta\tau$ and the optical anisotropy Δa of the PODIA chain segment are approximately twice as high as those of PTPMTPA in the same solvent [29]. One of the reasons is the negative contribution, which the phenylene side groups bring into the optical anisotropy of the PTPMTPA main chain (this fact follows, for instance, from the optical isotropy of the spherically symmetric tetraphenyl-methane group). This leads to the decrease in the total anisotropy of the macrochain unit length. In contrast, in PODIA molecule, the hexafluoroisopropylidene side substituents are optically isotropic units which do not bring a negative contribution into the anisotropy as it follows from the experimental data.

More rare including of the tetrahedron carbons into the PODIA chain (in comparison with PTPMTPA) is also significant. These groups do not bring a noticeable contribution into the chain anisotropy but bring a periodic kinks in the macromolecule direction (for a tetrahedron angle).

It was found that, in contrast to the stable state of PODIA in organic solvents, in 96% H_2SO_4 solution the polymer molecules are degradable, even at ambient temperature. Note that the PODIA chain consists formally of the PPOD and benzimide units linked by a hexafluoroisopropylidene group and the *p*-phenylene cycle. The PPOD in 96% H_2SO_4 solutions is stable at the same temperature as well as the benzimide units. We may refer, therefore, the hydrolytic instability of PODIA in concentrated sulphuric acid to the presence of the hexafluoroisopropylidene groups in the polymer chain. Recently, the similar lower thermal stability was mentioned for other polyimides with the additional methylene groups [38].

Acknowledgements

The authors are grateful for the financial support from the Deutschen Forschungsgemeinschaft through grant 436 Rus 113/107/R.

References

[1] Preston J. Aromatic polyamide fibers. Enc of pol sci a tech, Suppl., vol. 2. NY: Wiley; 1977. p. 84.
[2] Yang HH. Kevlar aramide fiber. Chichester: Wiley; 1991.
[3] Abade MJM, Sillion B. Polyimides and other high-temperature polymers. New York: Elsevier; 1991.
[4] Schulz B, Brehmer L. Poly(arylene-1,3,4-oxadiazole)s. In: Salamone JC, editor. Polymeric materials encyclopedia. New York: CRC Press; 1996.
[5] Arpin M, Strazielle C. Polymer 1977;18:591.
[6] Northdt MG. Polymer 1980;21:1199.
[7] Vitovskaya MG, Lavrenko PN, Okatova OV, Astapenko EP, Novakovsky VB, Bushin SV, Tsvetkov VN. Eur Polym J 1982;18: 583.
[8] Novakovsky VB, Lavrenko PN, Tsvetkov VN. Eur Polym J 1983;19: 931.
[9] Ying Q, Chu B, Qian R, Bao J, Zhang J, Xu C. Polymer 1985;26:1401.
[10] Jadhav JY, Kriogbaum WR, Preston J. Macromolecules 1988;21:538.
[11] Tsvetkov VN. Rigid-chain polymers. New York: Plenum Press; 1989.
[12] Lavrenko PN. Polymer 1990;31:1481.
[13] Lavrenko PN, Okatova OV, Garmonova TI, Cherkasov VA, Leibniz E, Schulz B. Eur Polym J 1995;29:893.
[14] Lavrenko PN. Polymer 1996;37:4409.
[15] Lavrenko PN, Pogodina NV. Macromolecules 1998;31:8831.
[16] Lavrenko PN, Okatova OV, Schulz B, Andreeva KA, Strelina IA. Eur Polym J 1999;35:655.
[17] Shifrina ZB, Averina MS, Rusanov AL, Wagner M, Müllen K. Macromolecules 2000;33:3525. Andreeva LN, Bushin SV, Belyaeva EV, Bezrukova MA, Averina MS, Keshtov ML, Shifrina ZB, Rusanov AL, Tsvetkov NV. Polym Sci (Engl Transl) 2002;44:141.
[18] Lavrenko PN, Strelina IA, Schulz B. Eur Polym J 1997;33:805.
[19] Lavrenko PN, Strelina IA, Okatova OV, Schulz B. Eur Polym J 2000; 36:1927.
[20] Korshak VV, Krongauz ES, Gribova IA, Krasnov AP, Sheina VE, Lioznov BS. Vysokomol Soyed (A) 1973;15:748.
[21] Song S-Y, Ahn T, Shim H-K, Song I-S, Kim W-H. Polymer 2001;42: 4803.
[22] Hergenrother PM. Am Chem Soc Polym Prepr 1978;19:40.
[23] Rusanov AL, Stadnik TA, Müllen K. Uspekhi Khimii 1999;68:760.
[24] Bruma M, Schulz B, Mercer F. The Third Euro Techn Symp on Polyimides STEPI 3. Montpellier, June; 1993
[25] Bruma M, Schulz B, Mercer FW. J Macromol Sci, Pure Appl Chem (A) 1995;32:259.
[26] Lavrenko PN, Okatova OV, Khokhlov KS. Instrum Exp Tech 1977;5: 208.
[27] Tsvetkov VN, Lavrenko PN, Bushin SV. J Polym Sci, Polym Chem Ed 1984;22:3447.
[28] Lavrenko PN, Okatova OV, Schulz B. Polym Sci (Engl Transl) (A) 1998;40:682.
[29] Cvetkov VN, Stennikova IN, Lavrenko PN, Kolbina GF, Okatova OV, Rafler G, Reinich G. Acta Polym 1980;31:434.
[30] Brocks G, Tol A. J Chem Phys 1997;106:6418.
[31] Lavrenko PN, Shtennikova IN, Garmonova TI, Mikrjukova OI, Gelmont MM, Efros LF. Polym Sci USSR (Engl Transl) 1986;28: 2335.
[32] Chiang R. J Polym Sci 1959;36:91.
[33] Lavrenko PN, Okatova OV. J Polym Sci, Polym Phys Ed 1993;31: 633.
[34] Benoit H. J Polym Sci 1948;3:376.
[35] Lavrenko PN, Okatova OV, Garmonova TI, Cherkasov VA, Leibniz E, Schulz B. Eur Polym J 1999;29:893.
[36] Shtennikova IN, Peker TV, Garmonova TI, Kolbina GF, Avrorova LV, Tokarev AV, Kudriavtsev GI, Tsvetkov VN. Vysokomol Soyed (A) 1981;23:2510.
[37] Strelina IA, Okatova OV, Lavrenko DM, Kolbina GF, Lavrenko PN. Vysokomol Soyed A 2003;45:71.
[38] Rusanov AL, Komarova LG, Prigozhina MP, Shevelev SA, Dutov MD, Serushkina OV. Vysokomol Soyed B 2002;44:2039.